ARTICLE

BIOTECHNOLOGY and BIOENGINEERING

Perfusion Flow Bioreactor for 3D In Situ Imaging: Investigating Cell/Biomaterials Interactions

J.S. Stephens, J.A. Cooper, F.R. Phelan Jr., J.P. Dunkers

Polymers Division, National Institute of Standards and Technology, 100 Bureau Dr, Gaithersburg, Maryland 20899; telephone: 301-975-6841; fax: 301-975-4977; e-mail: joy.dunkers@nist.gov

Received 18 July 2006; accepted 13 October 2006

Published online 5 December 2006 in Wiley InterScience (www.interscience.wiley.com). DOI 10.1002/bit.21252

ABSTRACT: The capability to image real time cell/material interactions in a three-dimensional (3D) culture environment will aid in the advancement of tissue engineering. This paper describes a perfusion flow bioreactor designed to hold tissue engineering scaffolds and allow for in situ imaging using an upright microscope. The bioreactor can hold a scaffold of desirable thickness for implantation (>2 mm). Coupling 3D culture and perfusion flow leads to the creation of a more biomimetic environment. We examined the ability of the bioreactor to maintain cell viability outside of an incubator environment (temperature and pH stability), investigated the flow features of the system (flow induced shear stress), and determined the image quality in order to perform time-lapsed imaging of two-dimensional (2D) and 3D cell culture. In situ imaging was performed on 2D and 3D, culture samples and cell viability was measured under perfusion flow (2.5 mL/min, 0.016 Pa). The visualization of cell response to their environment, in real time, will help to further elucidate the influences of biomaterial surface features, scaffold architectures, and the influence of flow induced shear on cell response and growth of new tissue.

Biotechnol. Bioeng. 2007;97: 952–961.

KEYWORDS: bioreactor; imaging; perfusion flow; tissue engineering

Introduction

The influence of biomaterial surface properties, chemical stimulation, and three-dimensional (3D) scaffold architecture on cell proliferation and differentiation are key elements in tissue engineering research (Griffith, 2002; Griffith and Naughton, 2002; Langer and Tirrell, 2004; Langer and Vacanti, 1993; Lu and Mikos, 1996). For example, specific surface chemistry can be used to maintain cell phenotype and promote differentiation (Griffith, 2000; Hench and Polak, 2002; Holmes, 2002; Shin et al., 2003). Physical characteristics, such as surface roughness, have also been shown to impact cell proliferation and differentiation, although the optimal surface roughness is cell type dependent (Flemming et al., 1999; Meredith et al., 2003; Simon et al., 2005; Washburn et al., 2004). The underlying reasons why surface chemistry and roughness are thought to influence cell function relates to their effects on protein adsorption and cellular adhesion (Flemming et al., 1999; Heilshorn et al., 2005; Koegler and Griffith, 2004; Lauffenburger and Griffith, 2001; Meredith et al., 2003; Simon et al., 2005; Stevens and George, 2005; Washburn et al., 2004). The pore size and interconnectivity of a tissue engineering scaffold also influences cellular activity, but again the optimal pore size and porosity are cell type dependent (Cukierman et al., 2001; Hollister, 2005; Karageorgiou and Kaplan, 2005; Zeltinger et al., 2001). Therefore processing tissue engineering scaffolds with proper pore size and interconnectivity is crucial for cell migration and survival.

More recently, research has focused on the effects of flow-induced shear stress on cell activity (Bancroft et al., 2002; Botchwey et al., 2003; Martin and Vermette, 2005; Minuth et al., 2000; Pathi et al., 2005; Yu et al., 2004). The addition of flow to in vitro culture environments is to create an environment that more closely mimics in vivo conditions. In vivo mechanotransduction is the process by which cells detect mechanical stimuli and translate them into biochemical signals. Shear stress is thought to be one of the most important mechanical stimuli for activating mechnotransduction (Liebschner, 2004; Sikavitsas et al., 2001; Vance et al., 2005; Weinbaum et al., 1994). Controlled flow systems, such as perfusion flow, spinner flasks, and

Correspondence to: J.P. Dunkers

rotary vessels, have shown increases in proliferation and differentiation for a variety of cell types (Botchwey et al., 2001; Goldstein et al., 2001; Hoerstrup et al., 2000; Lichtenberg et al., 2005). While all of these systems offer desirable flow features, the perfusion flow system enables flow through the interior of a 3D scaffold (Bancroft et al., 2002, 2003). The ability to flow media through the interior of the scaffolds leads to uniform cell coverage throughout the scaffold, a constant supply of nutrients, and the removal of metabolic waste (Bancroft et al., 2002, 2003; Cartmell et al., 2003; Pathi et al., 2005; Sikavitsas et al., 2005). Also, the use of perfusion flow bioreactors has shown significant increases in the associated phenotypic activity of osteoblasts through increased extracellular matrix and mineralized matrix production (Altman et al., 2002; Bancroft et al., 2002; Janssen et al., 2006; Wang et al., 2002).

The permeation of media through a scaffold or across a surface adds another layer of complexity in identifying the properties or combination of properties that are influencing cell response in these multi-component environments. Fixed time point analysis, such as common metabolic or protein assays and histology, have laid the foundation of understanding cell/cell, cell/substrate, and cell/scaffold interactions but only provide a "snapshot" of cellular response to the surrounding environment. Cells are dynamic, and the ability to collect time-lapsed live cell images of cell/cell and cell/material interactions, which lead to specific activities or events, such as proliferation, differentiation, or apoptosis, is of great interest (Beckman, 2003; Stephens and Allan, 2003; Thomas et al., 1996). Increasing knowledge about cell function in response to mechanical and chemical stimuli through time-lapsed imaging, and the ability to capture events as they unfold provides new levels of knowledge into cell function as a result of these outside influences (Beckman, 2003; Stephens and Allan, 2003; Thomas et al., 1996). The ability to image live cells in 3D scaffolds, under static and dynamic flow conditions, will aid in identification and optimization of the scaffold properties (surface chemistry and architecture) and flow conditions that enhance cell response.

Imaging in situ under physiologic conditions requires the use of a bioreactor. The bioreactor should be able to house both 3D scaffolds and 2D substrates and allow for perfusion flow. Bioreactors in general are designed to create microenvironments under which cells can be manipulated. Most of the perfusion flow bioreactors discussed in the literature have been developed, solely, for use in conventional humidified, 37°C, 5% by volume CO_2 cell culture incubators, which do not permit continuous imaging (Bancroft et al., 2003; Botchwey et al., 2001; Hoerstrup et al., 2000; Powers et al., 2002; Vance et al., 2005; Williams and Wick, 2004). The perfusion flow bioreactors that do allow for imaging are mainly designed for single cell evaluation or thin tissue samples (Focht, 1996; Hing et al., 2000). Bioreactors that hold thicker samples do not allow for perfusion (Czirok et al., 2002). Thicker scaffolds (>2 mm) are more relevant models for tissue repair (Laurencin et al., 1999). This paper describes the design and evaluation of a perfusion flow bioreactor for in situ imaging of 3D tissue engineering scaffolds. The parameters of the bioreactor that were evaluated include temperature and pH stability to ensure cell viability, flow rate measurements and flow profiles to determine flow induced shear stress, and 3D imaging capabilities under flow conditions.

Experimental Procedure

Conventional Cell Culture

MC3T3.E1 subclone 4 murine osteoblast cell line was purchased from American Type Culture Collection (ATCC, Arlington, VA). The cells were cultured in 75-cm^2 flasks using cell growth medium and maintained at 37°C in a humidified incubator at 5% by volume CO_2 environment. The cell growth medium was composed of alpha minimum essential medium (α-MEM), 10% fetal bovine serum (FBS) (Gibco/Invitrogen Corp., Grand Island, NY), 1% L-Glutamate (Cambrex/BioWhitaker, Walkersville, MD), 1% sodium pyruvate (Cambrex/BioWhitaker), and 1% penicillin/streptomycin (Fisher Scientific, Pittsburgh, PA). The medium was replaced every 3 days and cells between passage 4 and 8 were used.

Cell Viability in CO_2 Independent Medium

Imaging outside an incubator requires the maintenance of physiological pH under atmospheric CO_2 (<0.5%) conditions. To accomplish this, CO_2 independent medium (Gibco/Invitrogen Corp.) supplemented with 10% FBS, 1% L-Glutamate, and 1% antibiotic (penicillin/streptomycin) was used. Prior to imaging experiments, the passaged cells were resuspended in the CO_2 independent medium and plated (25 μL, 1×10^6 cells/mL) on a 6-well tissue culture polystyrene (TCPS). Each well was then filled with 2 mL of the CO_2 independent medium and cultured at 37°C under atmospheric CO_2 for 24 h. At (3, 6, 18, and 24) h time points a Live/Dead Viability/Cytotoxicity kit from Molecular Probes (calcein 494/517, ethidium homodimer-1 528/617) (Invitrogen) was used to evaluate cell viability, and the cells were imaged using the Nikon Eclipse TE 300 (Nikon, Melville, NY).

Bioreactor Design Parameters

The bioreactor was machined from medical grade stainless steel (316) and consists of a base and lid which screw together to close the cell growth chamber. Figure 1 is a schematic of the bioreactor design. A round 25 mm glass cover slip ($1\frac{1}{2}$ thickness, Fisher Scientific) is the window for imaging. Two silicone washers hold the cover slip in place between the lid and the base. The bioreactor is a closed loop system, and the cell growth medium is fed from a reservoir

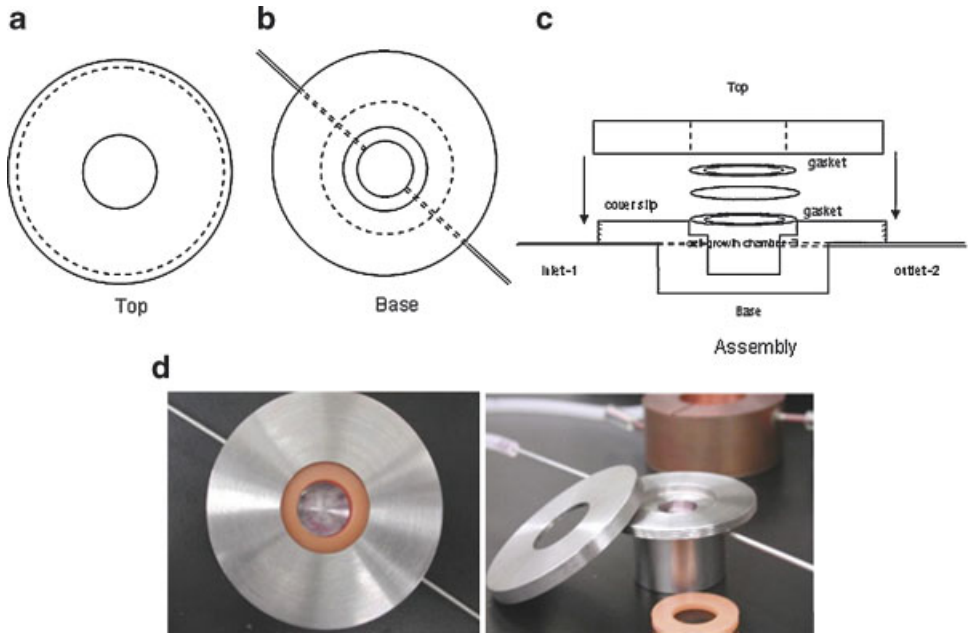

Figure 1. Bioreactor system. Schematic of (**a**) top (*d*: 57 mm), opening for viewing window (*d*: 20 mm), (**b**) base (*d*: 50 mm, *h*: 25 mm), (**c**) breakdown of the assembled bioreactor, 1—inlet (*d*: 1/16 in), 2—outlet (*d*: 1/16 in), 3—cell growth chamber (*d*: 12.5 mm, *h*; 3.5 mm), and (**d**) photograph of assembled and disassembled bioreactor. [Color figure can be seen in the online version of this article, available at www.interscience.wiley.com.]

bottle by a variable speed perfusion pump (Control Company, Friendswood, TX) through the cell growth chamber of the bioreactor and back to the reservoir bottle (see Fig. 2). The cell growth chamber is equipped with an inlet and an outlet for perfusion of the cell growth medium through the chamber. The tubing used to connect the system is peroxide cured silicone tubing with a 1/16 in (1.59 mm) inner diameter and a 3/16 in (4.76 mm) outer diameter (Master Flex, Cole Parmer, Vernon Hills, IL). This tubing was chosen because it is autoclavable and gas permeable.

Bioreactor Sterilization

To sterilize the bioreactor, the top, base, tubing, reservoir bottle, and cap were autoclaved (Napco, Hempstead, NY) together. The glass cover slip and silicone washers were sterilized by soaking in 70% volume fraction ethanol for 1 h, drying over night, ultraviolet (UV) irradiating for 15 min on each side, and triple rinsed with sterile Hanks Buffered Salt Solution (HBSS; Cellgro/Mediatech, Herndon, VA). The system was assembled in the cell culture hood to maintain sterility.

Testing Physiological Conditions Within the Bioreactor

A temperature of 37°C was maintained by housing the bioreactor and medium reservoir bottle in copper heating jackets, which were heated by flowing water from a circulation bath (Neslab, Waltham, MA). Figure 3 illustrates the heating jackets. The temperature stability of the specimen chamber was monitored continuously for 5 days using a thermocouple (Barnant Thermocouple Thermometer, Barrington, IL).

The pH of the cell growth medium was monitored using a pH meter (Oakton, Vernon Hills, IL), and measurements were taken every hour for the first 12 h and every 6–8 h for the next 48 h. An injection/withdrawal port was attached to the system for medium removal through out the investigation and to keep the system sterile.

Cell viability in the CO_2 independent medium (plus supplements) in static culture and in the bioreactor was evaluated using the Live/Dead Viability/Cytotoxicity Kit.

Imaging

The static culture imaging was done on a Nikon Eclipse TE 300. A Zeiss Laser Scanning Confocal Microscope (LSM) 510 (Zeiss, Heidelberg, Germany) was used to perform in situ imaging and to evaluate cell viability in the bioreactor. The LSM 510 was fitted with a C Achroplan NIR, 40×, water immersion, infinity and cover slip corrected objective with a 2 mm working distance and 0.8 numerical aperture (NA) (Zeiss). The Live/Dead Viability/Cytotoxicity Kit was also used for the in situ imaging investigations.

Image Fidelity

A 200-mesh transmission electron microscopy (TEM) grid (Electron Microscopy Sciences, Hatfield, PA) of known

DOI 10.1002/bit

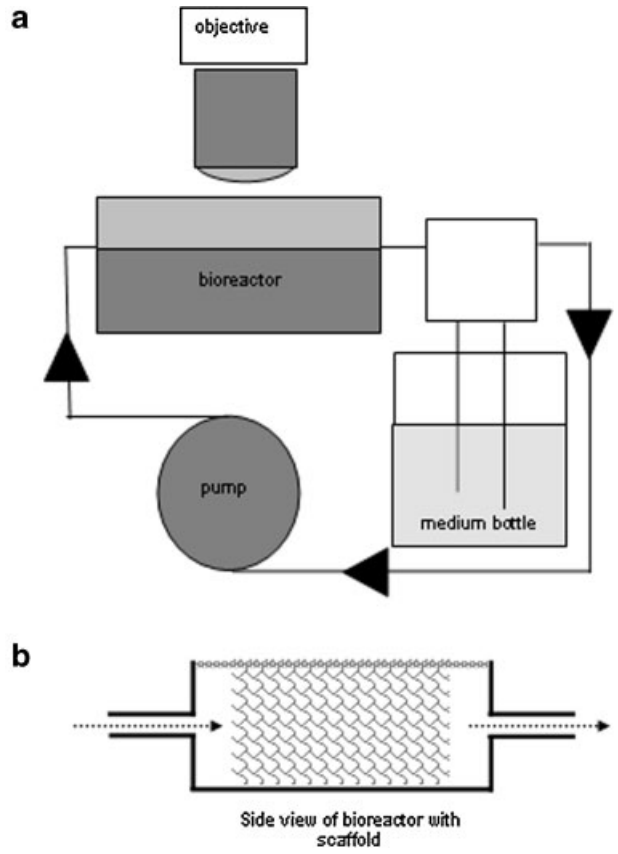

Figure 2. Illustration of closed loop system, (**a**) perfusion through bioreactor, arrows illustrate flow direction, and (**b**) perfusion through scaffold in the cell growth chamber.

spatial and geometric dimensions was imaged in air and in the bioreactor at various flow rates (<2.5 mL/min, 5.0 mL/min, and 8.5 mL/min) to evaluate the image fidelity of the bioreactor system under flow. The LSM 510 confocal with the 40×, cover-slip corrected, water immersion objective was used for imaging.

Flow Analysis

The flow rate through the bioreactor was measured using a flow meter (Omega, Stamford, CT). To ensure that the medium would perfuse through the entire volume of a scaffold in the bioreactor, a porous polymer salt leached scaffold was placed in the bioreactor under flow (2.5 mL/min). The scaffolds used were 84% porous photocured dimethacrylate salt leached scaffolds with an average pore size of 225 μm. The scaffold fabrication and characterization are described elsewhere (Landis et al., 2006). Briefly, the scaffolds used in these experiments, as well as for 3D in situ image, were made be salt leaching technique described by Landis et al. (2006). Briefly, a photocurable dimethacrylate polymer was mixed with 200–250 μm salt crystals. The mixture was then spread into mold, photocured on both sides, and soaked in deionized water to remove the salt particles. The scaffolds were cut to fit snugly into the bottom of the cell growth chamber of the bioreactor, and had a height of 3.0 mm and a diameter of 12.5 mm. The scaffolds were placed under flow in water and then an 8 μM rhodamine 123 in 50% (by mass fraction) ethanol solution (507/529) (Molecular Probes, Invitrogen) to visualize fluid permeation through the scaffold. The scaffold was imaged in 6 regions both before and after the addition of the Rhodamine 123 solution. To

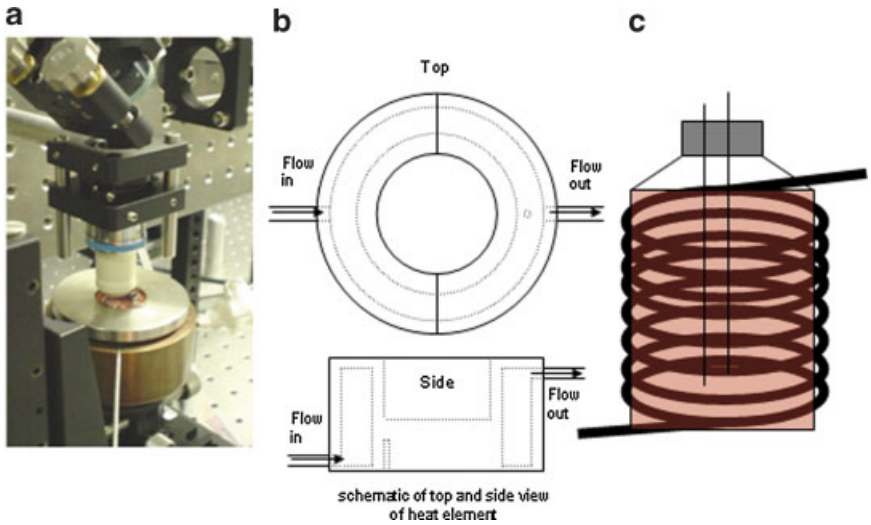

Figure 3. Heating system, (**a**) image of bioreactor in heating element on the microscope stage, (**b**) top and side view of copper water jacket machined to hold the bioreactor; and (**c**) pliable copper tubing was wrapped tightly around a 250 mL reservoir bottle and covered with insulation. Both heating elements were attached to the circulation bath (37°C) and the water was used to warm the medium and bioreactor. [Color figure can be seen in the online version of this article, available at www.interscience.wiley.com.]

assess flow perfusion, each of the 6 regions were imaged using the z-stack mode (10 μm/slice, 250 μm) on the Zeiss LSM 510 using the C Achroplan NIR, 40× objective.

The flow induced shear stress within the bioreactor was calculated using two approaches, a cylindrical pore model used by Goldstein et al. (2001) and a computational fluid dynamic (CFD) model. The cylindrical pore model estimates the shear stress with in a 3D scaffold and the CFD model calculates the shear stress within an empty bioreactor. For the CFD analysis, the governing equations used to model the flow are the steady Navier-Stokes equations together with the incompressible condition

$$\rho \underline{v} \cdot \nabla \underline{v} = -\nabla p + \eta \nabla^2 \underline{v}$$

$$\nabla \cdot \underline{v} = 0$$

where $\underline{v}$ is the velocity, p is the pressure, and η and ρ are the viscosity and density, respectively. Numerical solutions were obtained using the commercial finite element package COMSOL Multiphysics (COMSOL MP, Burlington, MA, 2006). Solutions reported here were obtained on a mesh consisting of 10,979 tetrahedral elements, with 52,220 total degrees of freedom.

2D Film and 3D Scaffold Preparation, Sterilization, and Culture

Poly (ε-caprolactone) (PCL) ($M_w = 80{,}000$), Scientific Polymer Products (Ontario, NY) films, approximately 1.5 mm thick, were used as a cell attachment substrate for the 2D in situ imaging trials. The scaffolds used for the 3D in situ imaging trials were the same as described in the flow study. The films and scaffolds were sterilized by soaking in 70% ethanol (volume fraction) for 1 h, dried over night, and UV irradiated on each side for 15 min. After UV irradiation, the films were triple rinsed with sterile α-MEM and then incubated in α-MEM for 30 min prior to cell seeding. The films and scaffolds were removed from the incubator and one film or scaffold was placed into each well of a 12-well TCPS plate. Each film was seeded drop-wise with 0.10 mL at 250,000 cells/mL. Each scaffold was seeded with 0.33 mL at 300,000 cells/mL. The cells were allowed to attach for 1 h in the incubator. After 1 h, 2 mL of α-MEM (plus supplements) was added to each well and the cells were incubated overnight. Following incubation, the respective specimens were removed from a well and placed into the cell growth chamber of the bioreactor for in situ imaging. The sample was covered with CO_2 independent medium and the chamber was closed and placed in the heating jacket. After 30 min, the perfusion pump was turned on (2.5 mL/min), and the system was inserted into the stage of the Zeiss LSM 510. Cell viability was assessed using a standard live/dead protocol. The flow was stopped and a 2 mL aliquot of medium containing the live/dead fluorophores was injected into the bioreactor. The fluorphore mixture was allowed to sit in the cell growth chamber for 10 min to stain the cells before the flow was started again (2.5 mL/min). The cells were imaged using the time-lapsed mode on the confocal. Images were collected every 5–10 min for 2–h.

Results and Discussion

The key elements of the bioreactor design are ease of use and the ability to perform live cell imaging while promoting healthy cellular activity outside of an incubator environment. Therefore, evaluating the temperature and pH stability, the image fidelity of the system, and the influence of flow and CO_2 independent cell growth medium on the cell viability are important factors in determining the usefulness of the bioreactor system.

The design parameters of the bioreactor also need to be addressed. The height of the bioreactor is a key element in its functionality and design; it must fit onto the stage of a conventional microscope. The system was designed for an upright microscope but could be modified for use on an inverted microscope. The height of the combined assembly (bioreactor in heating jacket) must provide enough clearance for the objective to pass over the surface. The total height is 30 mm, which leaves enough space to easily move the objective (Fig. 3). The imaging window is 20 mm in diameter, which provides adequate space for the objective to move across the desired viewing area. The cell growth chamber is 12.5 mm in diameter and 3.5 mm deep. A tissue engineering scaffold of these dimensions can be held tightly between the base and the lid or a film. It is important to ensure that the media is perfused through the scaffold and not around the periphery to attain the advantages of flow through the interior of the scaffold (Bancroft et al., 2003).

To measure the temperature and pH stability, the bioreactor was operated under cell culture conditions (perfusion flow and heated), placed on the lab bench, and monitored. The temperature stability of the system was monitored continuously over 5 days. A thermocouple was placed in the cell growth chamber and the medium exchange bottle. Once the temperature system reached 37°C, the temperature remained stable at 37 ± 1°C over the 5 days period. This approach was taken because the heating system is completely separate from the bioreactor and does not need to be kept sterile.

To perform in situ imaging using the bioreactor, the cell growth medium has to maintain a stable pH (7.4) under atmospheric CO_2 (<0.5%). To investigate the pH stability of the CO_2 independent cell growth medium, the bioreactor was sterilized and set-up to run. The pH of the medium under perfusion flow at 37°C was stable at 7.3 (±0.1) over the 48 h investigation. It was assumed that the pH would remain stable over the time the imaging experiments would be run, since up to 48 h there was no variation in the pH. This investigation also showed that the bioreactor maintains a sterile environment.

DOI 10.1002/bit

The flow rate was measured as the media was perfusing out of the cell growth chamber and back through the tubing. The flow rates were measured for both an empty chamber and a chamber containing a porous scaffold (84% porosity). This porosity was chosen because it is a common porosity for tissue engineering scaffolds (Bancroft et al., 2003; Karageorgiou and Kaplan, 2005). The flow rates did not change considerably between the empty and filled chamber (Table I). The flow rates measured for this bioreactor are higher than those reported in the literature (Bancroft et al., 2002; Cartmell et al., 2003; Vance et al., 2005; Wang et al., 2002); 4.34–8.18 mL/min versus 0.01–3 mL/min, respectively. The lower flow rates, <3 mL/min, were not detectable by the flow meter. This lower range is estimated to have a flow rate of approximately 2.5 mL/min and was used in the in situ imaging trials.

Figure 4a illustrates the flow through the cell growth chamber. The chamber fills in a matter of seconds and good dissemination of the green fluid results. The perfusion of the media through a scaffold (84% porous, *h*: 3.0 mm, *d*: 12.5 mm) in the bioreactor was investigated using the confocal and a fluorescent solution (rhodamine 123). The scaffold was imaged using the z-stack mode (*z*: 250 μm) in six regions, representing the entire scaffold. The scaffold was first imaged under flow in water and showed no fluorescence. The fluorophore solution was then perfused through the scaffold and imaging confirmed that all sections of the scaffold were stained with the fluorophore (data not shown). This is a good indication that the bioreactor promotes perfusion through the entire scaffold, rather than only around the periphery.

In order to relate the flow rate to shear stress, a cylindrical pore model used by Goldstein et al. (2001) and a CFD model were used to calculate the shear stress within the bioreactor. The cylindrical pore model estimates the shear stress (τ_w) felt by the cell within the scaffold

$$\tau_w = (8\mu V_m)/d$$

where μ is the viscosity (0.01 dyn s/cm^2), V_m is the mean velocity, and d is the mean pore size (200 μm). To calculate V_m

$$V_m = \frac{Q}{[\Phi\pi(D/2)^2]}$$

Table I. Flow rates through the chamber, with and without scaffold.

Setting	Flow rate (w/scaffold) (mL/min)	Flow Rate (w/o scaffold) (mL/min)
Slow, 10	6.56	8.01
Slow, 5	5.26	6.18
Slow, 0	[a]	4.34
Fast, 10	7.30	8.18
Fast, 5	5.26	6.56
Fast, 0	[a]	4.80

[a]Flow was too low to be measured.

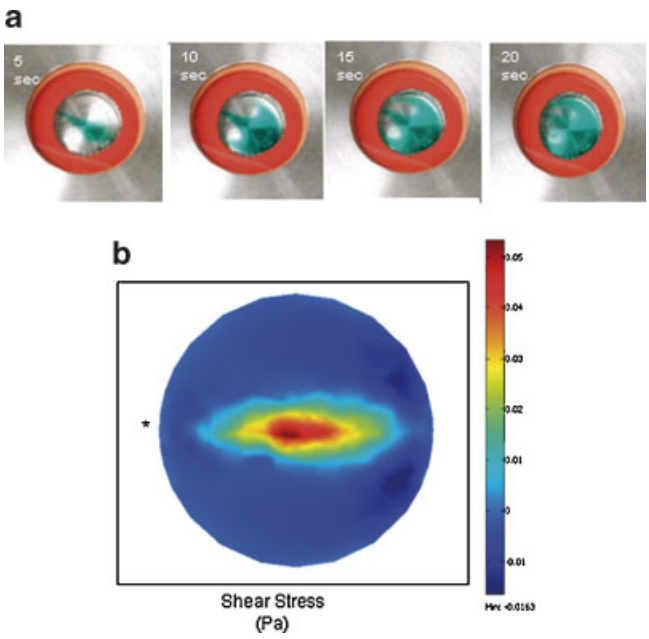

Figure 4. Perfusion flow analysis, (**a**) the medium flowing in from the upper left corner and out through the lower right corner. These images show that the liquid (green) enters the chamber and mixes thoroughly (clear to green). **b**: CFD model of flow induced shear stress at the bottom the cell growth chamber, ranging from 0.05 to 0.01 Pa, with an average of 0.016 (*inlet). Note that the shear stress is a tensor quantity and therefore can be positive or negative depending on direction of the velocity vector. [Color figure can be seen in the online version of this article, available at www.interscience.wiley.com.]

where *Q* is the flow rate (2.5 mL/min), *Φ* is the scaffold porosity (84%), and *D* is the scaffold diameter (12.5 mm). The calculated shear stress (τ_w) felt by the cells within the scaffold is 0.016 Pa. The CFD model calculated the shear stress at the lower surface of the cell growth chamber, Figure 4B, for an empty chamber. The shear stress ranged from 0.05 to 0.01 Pa; note these are tensor values with negative and positive values resulting from the direction of the velocity vector. The highest stress is located at the center of the chamber due to the flow through the inlet and outlet valves. However, the majority of the contents within the cell growth chamber would feel a shear stress between 0.02 and 0.01 Pa. These shear stress values correspond directly to those calculated using the cylindrical pore model above. These values are 2 orders of magnitude lower than flow induced shear stress felt in vivo (0.8–3.0 Pa), but are comparable to shear stress values reported in the literature (Bancroft et al., 2002; Goldstein et al., 2001; Gomes et al., 2003; Sikavitsas et al., 2005; Vance et al., 2005). Shear stress levels in this range have been shown the increase gene expression and ECM production (Bancroft et al., 2002; Botchwey et al., 2001; Porter et al., 2005; Sikavitsas et al., 2005; Vance et al., 2005). Also, the Reynolds number (Re) at the inlet valve, Re = 38, and within the center of the cell growth chamber, Re = 355. This increase in Re indicates that the medium is mixing within the cell growth chamber. These

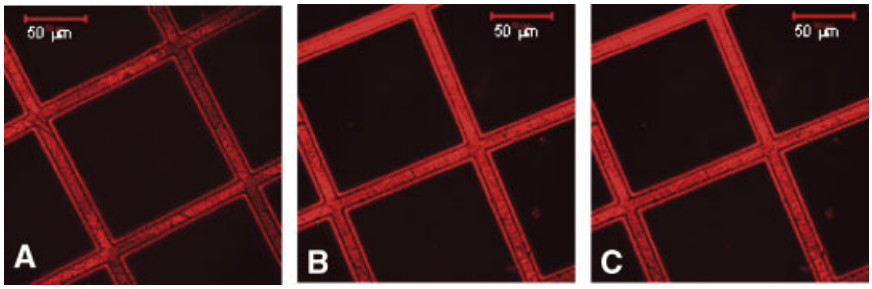

Figure 5. Image fidelity, 200 mesh TEM grid in bioreactor, (**a**) static, (**b**) low flow, ~2.5 mL/min, and (**c**) high flow, ~8 mL/min. Scale bar, 50 μm. [Color figure can be seen in the online version of this article, available at www.interscience.wiley.com.]

findings support the flow visualizations observed in the Figure 4a and described further in the fluorescence flow investigation. Therefore, this bioreactor system possesses flow parameters that are conducive to increasing cell response due to flow induced shear stress.

To qualitatively assess the fidelity of the image to the structure inside the bioreactor, a 200 mesh TEM grid was imaged under static conditions and flow rates of 2.5, 5.0, and 8.5 mL/min. The TEM grid was chosen because its regularly spaced features are on the same size scales as the cells (10–20 μm) and the scaffolds (>100 μm). The identical microscope set-up used was also used in the in situ imaging trials. Figure 5 shows the images under static conditions and flow rates of 2.5 mL/min and 8.5 mL/min. No changes were seen in the image quality indicating that the image quality within the bioreactor remains constant regardless of flow rate.

The cell viability in the CO_2 independent cell growth medium was monitored at 3, 6, 18, and 24 h. At each time point, the viability assay indicated that the cells were viable. Figure 6a shows the images taken after 18 h in CO_2 independent cell growth medium under atmospheric CO_2. These images, taken on the Nikon, are representative of all the time points. Figure 6b shows the results from the viability assay (green—viable, red—apoptotic). The cells remained viable over the course of the investigation, confirming that the CO_2 independent cell growth medium can sustain viable cells.

The last step in testing the design of the bioreactor is to perform in situ imaging evaluations. These investigations will indicate imaging feasibility in 2D and 3D by verifying the viability under flow conditions at 2.5 mL/min. For both the 2D films and the 3D scaffolds, images were collected in 5 min or 10 min time intervals for each 2 or 4 h period. After each imaging set (2 or 4 h) the samples were evaluated to determine photo bleaching and cell damage. If the cells still appeared to be viable (i.e., green) then another set of time-lapsed images was collected. Figure 7 shows a series of images taken on a 2D film under flow (2.5 mL/min) every 5 min over a 2 h time period. These image sets were collected after the film had been in the bioreactor for 4 h. The time on the images indicates when they were taken in the series, that is, 5 min from start of image series. This image set shows cell movement on the surface of the PCL film under flow. A time-lapsed movie is included to better demonstrate cell motility. These experiments indicate that the cells remain

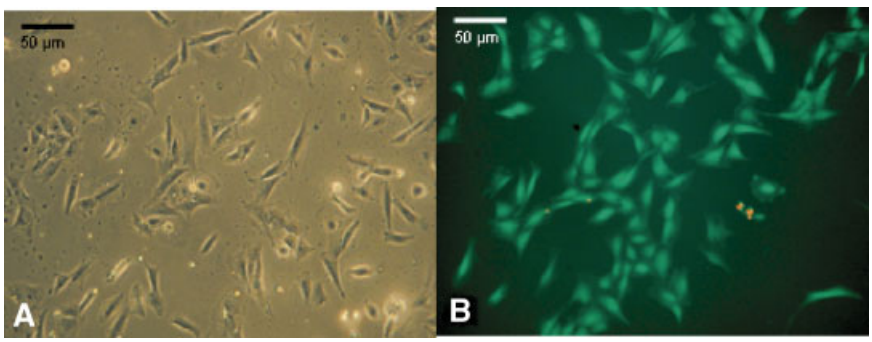

Figure 6. Cell viability in CO_2 independent cell growth medium, (**a**) optical image of cells, shows a healthy morphology, (**b**) live/dead assay, green—viable, red—apoptotic. [Color figure can be seen in the online version of this article, available at www.interscience.wiley.com.]

DOI 10.1002/bit

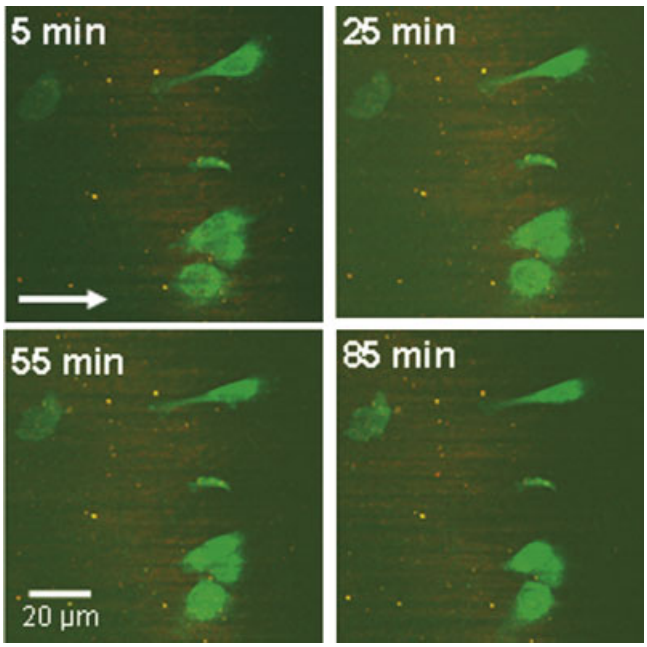

Figure 7. 2D in situ imaging trial. The cells were incubated in the bioreactor for over 4 h before images were collected. The time lapsed images show cell movement on the surface of the PCL film and as a result of the flow conditions. The white arrow indicates flow direction. From the live/dead assay green cells indicate that the cells are viable over the 2 h the images were acquired. [Color figure can be seen in the online version of this article, available at www.interscience.wiley.com.]

viable under flow and that time-lapsed imaging is possible using this bioreactor system. The final step was to determine feasibility of 3D in situ imaging.

Figure 8 depicts a series of images collected during the 3D scaffold in situ imaging trial. The scaffold had been in the bioreactor for 2 h when the image collection was started, and a new set of images were captured every 10 min over the next 3 h. Although this imaging set was only collected over 3 h, viable cells were seen up to 18 h after the scaffold was placed in the bioreactor. The images were collected 100 μm below the surface of the scaffold. This image series demonstrates the ability to image viable cells and movement on the irregular surface of a pore wall. Also, a supplemental movie is included showing cells were imaged up to 180 μm deep into the interior of the scaffold. The movie begins at the edge of a pore on the surface. As the imaging progresses deeper into the scaffold, the empty pore space is reflected by a features image. Nearing the bottom of the pore, cells bridging the pore walls are evident. These investigations demonstrate the capabilities of the design of an in situ imaging, perfusion flow bioreactor for imaging of 3D tissue engineering scaffolds.

Conclusions

The goal of tissue engineering is to create materials, scaffolds, and in vitro culture environments that invoke biomimetic cell response. Traditional end point investigations have been important in developing an understanding of cell/material interactions. However they do not tell the complete story. In this work, we demonstrate a perfusion flow bioreactor with 3D in situ imaging capabilities for continuous monitoring of cell response. The physiological conditions (temperature, pH, and flow) of the bioreactor were tested and showed that it maintained cell viability. The flow conditions and the corresponding flow induced shear stress were analyzed to reveal good mixing within the bioreactor. The average shear stress values (0.01–0.02 Pa) compares well with values shown to increase osteoblast gene expression and production of mineralized matrix (Bancroft et al., 2002; Botchwey et al., 2001; Porter et al., 2005; Sikavitsas et al., 2005; Vance et al., 2005). The final step in evaluating the bioreactor was to perform 3D in situ imaging. These cells remained viable within the scaffold and under flow demonstrating that 3D in situ imaging is possible with this bioreactor system. Real time analysis of cell/material interactions in 3D tissue engineering scaffolds will continue to reveal the influences of scaffold architecture on cellular activity.

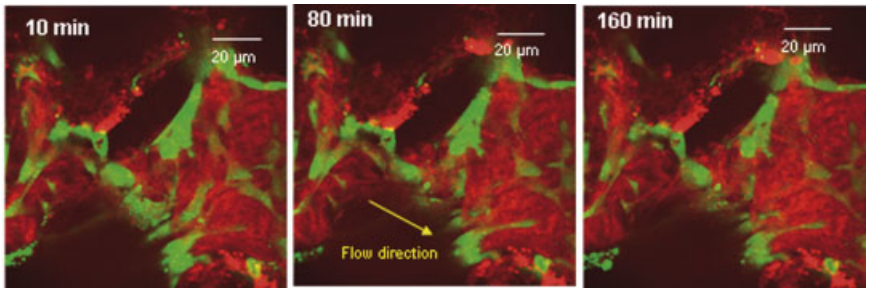

Figure 8. 3D in situ imaging trial. Images were collected over a 3 h time period. The scaffold is shown in red (reflection mode, false color) and the cells are a stained green (calcein), indicating they are viable. The yellow arrow indicates the direction of flow. [Color figure can be seen in the online version of this article, available at www.interscience.wiley.com.]

The authors would like to acknowledge CR Snyder for assistance in heating element design and ML Becker for useful discussions. We would also like to thank the Fabrication Technology Division for help constructing the bioreactor. JS Stephens would like to acknowledge a fellowship from the NIST/NRC Research Assistantship Program.

References

Altman GH, Horan RL, Martin I, Farhadi J, Stark PRH, Volloch V, Richmond JC, Vunjak-Novakovic G, Kaplan DL. 2002. Cell differentiation by mechanical stress. FASEB J 16:270–272.

Bancroft GN, Sikavitsast VI, van den Dolder J, Sheffield TL, Ambrose CG, Jansen JA, Mikos AG. 2002. Fluid flow increases mineralized matrix deposition in 3D perfusion culture of marrow stromal osteloblasts in a dose-dependent manner. Proc Natl Acad Sci USA 99:12600–12605.

Bancroft GN, Sikavitsas VI, Mikos AG. 2003. Design of a flow perfusion bioreactor system for bone tissue-engineering applications. Tissue Eng 9:549–554.

Beckman M. 2003. Play-by-play imaging rewrites cells' rules. Science 300: 76–77.

Botchwey EA, Pollack SR, Levine EM, Laurencin CT. 2001. Bone tissue engineering in a rotating bioreactor using a microcarrier matrix system. J Biomed Mater Res 55:242–253.

Botchwey EA, Dupree MA, Pollack SR, Levine EM, Laurencin CT. 2003. Tissue engineered bone: Measurement of nutrient transport in three-dimensional matrices. J Biomed Mater Res Part A 67A:357–367.

Cartmell SH, Porter BD, Garcia AJ, Guldberg RE. 2003. Effects of medium perfusion rate on cell-seeded three-dimensional bone constructs in vitro. Tissue Eng 9:1197–1203.

Cukierman E, Pankov R, Stevens DR, Yamada KM. 2001. Taking cell-matrix adhesions to the third dimension. Science 294:1708–1712.

Czirok A, Rupp PA, Rongish BJ, Little CD. 2002. Multi-field 3D scanning light microscopy of early avian embryogenesis at cellular resolution. Mol Biol Cell 13:551A.

Flemming RG, Murphy CJ, Abrams GA, Goodman SL, Nealey PF. 1999. Effects of synthetic micro- and nano-structured surfaces on cell behavior. Biomaterials 20:573–588.

Focht DC. 1996. Live-cell microscopy: Environmental control for mammalian specimens. Nat Biotechnol 14:361–362.

Goldstein AS, Juarez TM, Helmke CD, Gustin MC, Mikos AG. 2001. Effect of convection on osteoblastic cell growth and function in biodegradable polymer foam scaffolds. Biomaterials 22:1279–1288.

Gomes ME, Sikavitsas VI, Behravesh E, Reis RL, Mikos AG. 2003. Effect of flow perfusion on the osteogenic differentiation of bone marrow stromal cells cultured on starch-based three-dimensional scaffolds. J Biomed Mater Res Part A 67A:87–95.

Griffith LG. 2000. Polymeric biomaterials. Acta Materialia 48:263–277.

Griffith LG. 2002. Emerging design principles in Biomaterials and scaffolds for tissue engineering. Reparative Med Growing Tissues Organs 961: 83–95.

Griffith LG, Naughton G. 2002. Tissue engineering—Current challenges and expanding opportunities. Science 295:1009-+.

Heilshorn SC, Liu JC, Tirrell DA. 2005. Cell-binding domain context affects cell behavior on engineered proteins. Biomacromolecules 6:318–323.

Hench LL, Polak JM. 2002. Third-generation biomedical materials. Science 295:1014.

Hing WA, Poole CA, Jensen CG, Watson M. 2000. An integrated environmental perfusion chamber and heating system for long-term, high resolution imaging of living cells. J Microsc Oxf 199:90–95.

Hoerstrup SP, Sodian R, Sperling JS, Vacanti JP, Mayer JE. 2000. New pulsatile bioreactor for in vitro formation of tissue engineered heart valves. Tissue Eng 6:75–79.

Hollister SJ. 2005. Porous scaffold design for tissue engineering. Nature Mater 4:518–524.

Holmes TC. 2002. Novel peptide-based biomaterial scaffolds for tissue engineering. Trends Biotechnol 20:16–21.

Janssen FW, Oostra J, van Oorschot A, van Blitterswijk CA. 2006. A perfusion bioreactor system capable of producing clinically relevant volumes of tissue-engineered bone: In vivo bone formation showing proof of concept. Biomaterials 27:315–323.

Karageorgiou V, Kaplan D. 2005. Porosity of 3D biornaterial scaffolds and osteogenesis. Biomaterials 26:5474–5491.

Koegler WS, Griffith LG. 2004. Osteoblast response to PLGA tissue engineering scaffolds with PEO modified surface chemistries and demonstration of patterned cell response. Biomaterials 25:2819–2830.

Landis FA, Stephens JS, Cooper J, Cicerone MT, Lin-Gibson S. 2006. Tissue engineering scaffolds based on photocured dimethacrylate polymers for the in vitro optical imaging of cellular activity. Biomacromolecules 7: 1751–1757.

Langer R, Tirrell DA. 2004. Designing materials for biology and medicine. Nature 428:487–492.

Langer R, Vacanti JP. 1993. Tissue engineering. Science 260:920–926.

Lauffenburger DA, Griffith LG. 2001. Who's got pull around here? Cell organization in development and tissue engineering. Proc Natl Acad Sci USA 98:4282–4284.

Laurencin CT, Ambrosio AMA, Borden MD, Cooper JA. 1999. Tissue engineering: Orthopedic applications. Annu Rev Biomed Eng 1:19–46.

Lichtenberg A, Dumlu G, Walles T, Maringka M, Ringes-Lichtenberg S, Ruhparwar A, Mertsching H, Haverich A. 2005. A multifunctional bioreactor for three-dimensional cell (co)-culture. Biomaterials 26: 555–562.

Liebschner MAK. 2004. Biomechanical considerations of animal models used in tissue engineering of bone. Biomaterials 25:1697–1714.

Lu LC, Mikos AG. 1996. The importance of new processing techniques in tissue engineering. MRS Bulletin 21:28–32.

Martin Y, Vermette P. 2005. Bioreactors for tissue mass culture: Design, characterization, and recent advances. Biomaterials 26:7481–7503.

Meredith JC, Sormana JL, Keselowsky BG, Garcia AJ, Tona A, Karim A, Amis EJ. 2003. Combinatorial characterization of cell interactions with polymer surfaces. J Biomed Mater Res Part A 66A:483–490.

Minuth WW, Schumacher K, Strehl R, Kloth S. 2000. Physiological and cell biological aspects of perfusion culture technique employed to generate differentiated tissues for long term biomaterial testing and tissue engineering. J Biomater Sci Polym Ed 11:495–522.

Pathi P, Ma T, Locke BR. 2005. Role of nutrient supply on cell growth in bioreactor design for tissue engineering of hematopoietic cells. Biotechnol Bioeng 89:743–758.

Porter B, Zauel R, Stockman H, Guldberg R, Fyhrie D. 2005. 3-D computational modeling of media flow through scaffolds in a perfusion bioreactor. J Biomech 38:543–549.

Powers MJ, Domansky K, Kaazempur-Mofrad MR, Kalezi A, Capitano A, Upadhyaya A, Kurzawski P, Wack KE, Stolz DB, Kamm R, Griffith LG. 2002. A microfabricated array bioreactor for perfused 3D liver culture. Biotechnol Bioeng 78:257–269.

Shin H, Jo S, Mikos AG. 2003. Biomimetic materials for tissue engineering. Biomaterials 24:4353–4364.

Sikavitsas VI, Temenoff JS, Mikos AG. 2001. Biomaterials and bone mechanotransduction. Biomaterials 22:2581–2593.

Sikavitsas VI, Bancroft GN, Lemoine JJ, Liebschner MAK, Dauner M, Mikos AG. 2005. Flow perfusion enhances the calcified matrix deposition of marrow stromal cells in biodegradable nonwoven fiber mesh scaffolds. Ann Biomed Eng 33:63–70.

Simon CG, Eidelman N, Kennedy SB, Sehgal A, Khatri CA, Washburn NR. 2005. Combinatorial screening of cell proliferation on poly(D, L-lactic acid)/poly(D, L-lactic acid) blends. Biomaterials 26:6906–6915.

Stephens DJ, Allan VJ. 2003. Light microscopy techniques for live cell imaging. Science 300:82–86.

Stevens MM, George JH. 2005. Exploring and engineering the cell surface interface. Science 310:1135–1138.

Thomas C, De Vries P, Hardin J, White J. 1996. Four-dimensional imaging: Computer visualization of 3D movements in living specimens. Science 273:603.

DOI 10.1002/bit

Vance J, Galley S, Liu DF, Donahue SW. 2005. Mechanical stimulation of MC3T3 osteoblastic cells in a bone tissue-engineering bioreactor enhances prostaglandin E-2 release. Tissue Eng 11:1832–1839.

Wang Y, Uemura T, Dong J, Kojima H, Tateishi T. 2002. Perfusion culture system improves osteogenesis of rat bone marrow derived osteoblastic cells in porous ceramic materials. J Bone Miner Res 17: S338.

Washburn NR, Yamada KM, Simon CG, Kennedy SB, Amis EJ. 2004. High-throughput investigation of osteoblast response to polymer crystallinity: Influence of nanometer-scale roughness on proliferation. Biomaterials 25:1215–1224.

Weinbaum S, Cowin SC, Zeng Y. 1994. A model for the excitation of osteocytes by mechanical loading-induced bone fluid shear stresses. J Biomech 27:339–360.

Williams C, Wick TM. 2004. Perfusion bioreactor for small diameter tissue-engineered arteries. Tissue Eng 10:930–941.

Yu XJ, Botchwey EA, Levine EM, Pollack SR, Laurencin CT. 2004. Bioreactor-based bone tissue engineering: The influence of dynamic flow on osteoblast phenotypic expression and matrix mineralization. Proc Natl Acad Sci USA 101:11203–11208.

Zeltinger J, Sherwood JK, Graham DA, Mueller R, Griffith LG. 2001. Effect of pore size and void fraction on cellular adhesion, proliferation, and matrix deposition. Tissue Eng 7:557–572.